



## HEAT TRANSFER ANALYSIS AND TURBULENCE MODELS INVESTIGATION OF NUCLEATE BOILING FLOW IN NUCLEAR REACTOR APPLICATION

Magdi Saad Farag Ali<sup>1i</sup>,

Hani Saed Faraj Ali<sup>2</sup>

<sup>1</sup>Universiti Tun Hussein Onn Malaysia (UTHM),  
Malaysia

<sup>2</sup>Department of Electronics and Computer Engineering,  
Bilecik Şeyh Edebali University,  
Bilecik, Turkey

### Abstract:

Boiling water exhibits an exceptionally high heat transfer coefficient, making it a valuable tool across numerous applications. However, once the heat flux surpasses a certain elevated threshold, the heated surface can no longer sustain continuous liquid contact. This is associated with a significant decline in heat transfer efficiency. The result may be a sudden spike in surface temperature within a heat flux-controlled system, or a dramatic decrease in power transferred in a temperature-controlled system. In the present study, the heat flux has been investigated in a circular channel heated by two roads. Parameters with emphasis on water flow velocity correlated with different heat transfer values from the roads. The methodology contains both laboratory experiments and a simulation model. The obtained results indicate that different heating surfaces play an important role in boiling heat transfer. Also, there is a clear relationship between the water flow and surface temperature. The amount of absorbed temperature increases by about 13% in a flow of 0.45 m/s. while in the water flow velocity 0.89 m/s and 1.34 m/s vary to 16.3% and 17% respectively. The other impressive result is the phenomenon of alternate water temperature values due to certain regional temperatures. It's observed that there is a difference in heat absorption based on the amount of heat flux from the surface. The general rate of heat flux in the system was 6736.557 W/1°C for each square meter of heat generation. The obtained information is useful in controlling the boiling water reactor from sudden shutdown and also in controlling the boundaries in the design phase.

**Keywords:** nuclear reactor, heat transfer, boiling flow, turbulence models, heat flux, temperature distribution

---

<sup>i</sup> Correspondence: email [magdialzway2000@gmail.com](mailto:magdialzway2000@gmail.com)

## 1. Introduction

The development of nuclear reactors paved the way for coolant application studies, which have become an important issue due to the significance of boiling point phenomena. This represents one of the major factors in reactor design. It is interesting to consider the boiling conditions in the event of loss of coolant during regular operation. Boiling point phenomena impact the heat transfer coefficient and are therefore employed in many engineering applications.

One of the boiling phenomena is Nucleate Boiling, which occurs when the surface temperature is hotter than the saturated fluid temperature. This is the most effective heat transfer method because of its high performance stemming from latent heat transport, thus reducing the size, weight and volume of heat exchange devices and improving thermal performance.

The nature of nucleate pool boiling is a non-equilibrium process, where a heated solid transfers heat to the fluid adjacent to the surface. The precise details of each part of the full cycle are quite complicated, but it has become common to divide the cycle into several distinct stages. These stages contain the superheated thermal layer in the liquid near the heated surface, as well as thermal and mechanical equilibrium (Sateesh & Balakrishnan, 2005).

In recent years, scholars have reconsidered water as a kind of natural coolant that is environmentally friendly, safe, and cheap. The systems of using water as a coolant run at specific conditions that generate combined properties of the fluid behaviour that need to be determined, with each case requiring the identification of the most significant parameter. During the interaction of heat transfer, the thermal limit phase changes to reach the critical heat flux. This phenomenon decreases the efficiency of heat transfer and causes localized overheating of the heating surface. To desirable the operation of the boiling process, the boiling curve can observe a great means of heat transfer. It specifies the critical heat flux, which represents an important point in the heat transfer behaviour.

### 1.1 Background

In a nuclear power plant, the fission process, as a means to generate energy, turns a generator by a stream of steam. The fission process takes place in the reactor. There are several different types of nuclear reactors, the most common of which are pressurized water reactors and boiling water reactors (Thom *et al.*, 1965).

In nuclear reactor operations, maintaining a zero-reactivity balance ensures steady power output. When reactivity shifts positively, power levels rise, whereas negative reactivity results in declining power output. The reactivity balance equation incorporates several key variables, including the temperature and density of water, fuel element temperature, and core void formation (Graham, 2012). During transient conditions, the precision of core power calculations depends heavily on the measurement accuracy of these individual parameters.

With the advent of technology, nucleate boiling phenomena have become an effective factor in liquid-cooled devices. The heat flux generated by various devices is increasing exponentially. Therefore, cooling these devices has become very essential and a matter of serious consideration. A typical boiling curve illustrates the different boiling regimes for a given temperature increment (Shah, 1977; Rainey & You, 2001).

## 1.2 Problem Statement

In Boiling Water Reactor (BWR) systems, electrical power generation occurs through a direct process where light water transitions to steam within the reactor vessel before driving the turbine assembly. Operational challenges arise from inherent instabilities caused by fluctuating density patterns and thermal-hydraulic response mechanisms. The dual role of water as both coolant and neutron moderators creates a complex dynamic - variations in core void distributions influence both neutron flux patterns and power generation rates. These changes subsequently modify void fraction characteristics (Shah, 1976).

This interconnected behaviour leads to distinct categories of thermal-hydraulic instability phenomena within BWR systems (Dokhane, 2004). The parameters which affect the stability behaviour of the BWR can be described as Mass flow, Inlet sub-cooling, System Pressure, Inlet and exit pressure drop, Length of the channel, Core power, Axial power shape, Void reactivity coefficient, Radial power shape (Amselem Abecasis, 2010). In addition to those previous parameters, there are thermal-hydraulic properties and dimensionless numbers that could be related to stability behaviour (Shoji, 2004).

The challenge is how to investigate the methods that will help to predict and avoid instability-related shutdowns. For that purpose, thermal hydraulics simulation tools can be used to extract real Boiling Water Reactors (BWR) data. This data will be analysed and used to predict the plant's stability behaviour.

Finally, the experimental approach to the problem may lead to a satisfactory solution at a reasonable cost and time, so we should hold numerically accurate simulations of the flow and heat transfer through Boiling Water Reactors (BWR) to achieve efficient behaviour.

In the functioning of nuclear reactors, heat transfer processes must be optimal, not only for the energy efficiency of the reactor but also to ensure its safety and life span. Efficient means of cooling lessen the overheating risks that may result in erosion of reactor materials, the boiling crisis of coolants, damper cases, and damage to the reactor core. With nuclear energy being essential as an option for the world's growing energy needs, the issue of thermal stability considering different working situations became more pressing. Newer generations of reactors were designed to incorporate increased capabilities to cool the systems, improve their output, and extend the periods of trouble-free operation. More so, the attention paid in this study to the patterns of heat fluxes and water circulations is topical, as it concerns the tendencies towards the enhancement of safety and efficiency of the reactors in operation.

## 2. Literature Review

### 2.1 Introduction

Heat transfer has been an interesting subject for scientists and researchers in the past decades. Numerical and experimental studies have been reported to enhance a good understanding of heat transfer behaviour. The major important heat transfer phenomenon in the reactors is water boiling, which represents the rapid vaporization of the water inside the reactor. Boiling incipience strongly depends on the saturation wall superheat, among other factors. Understanding wall superheat heat flux characteristics, therefore, emerges as a critical research priority.

The dynamics of boiling processes have attracted sustained attention from research teams and engineering professionals across global institutions. Investigators have approached this field through parallel paths of computational analysis and laboratory experimentation, generating extensive technical literature. Our analysis focuses particularly on research examining curved surface interactions, aligning with the central objectives of this investigation (Yamamoto *et al.*, 2005; Kataoka *et al.*, 1992).

### 2.2 BWR Overview

BWR technology was initiated in 1955 with an inaugural design comprising experimental configurations of both dual-cycle and direct-cycle systems. The distinguishing feature between these variants lay in the dual-cycle's incorporation of steam generation equipment.

By 1963, the second-generation BWR emerged, emphasizing streamlined direct-cycle architecture and standardized design principles. This iteration introduced integrated steam separation mechanisms and employed five peripheral recirculation circuits. The system's load-following capabilities relied on adjustable-speed recirculation pump technology (Saha, 1977).

A significant advancement arrived in 1965 with the third-generation design, characterized by the integration of internal jet pump technology for recirculation enhancement. This innovation permitted a reduction in recirculation circuit quantity and enabled smaller diameter piping, as the operational requirements decreased to approximately one-third of total core flow under rated conditions (Halsall, 1977; Saha 1977).

The fourth-generation BWR, unveiled in 1966, focused primarily on enhancing core power density capabilities.

In 1969, the fifth-generation design brought substantial revisions to safety and circulation systems. Key improvements included enhanced Emergency Core Cooling System (ECCS) configurations and modernized recirculation mechanisms. The design shifted from variable-speed pump technology to an integrated system of flow-control valves working in conjunction with fixed-speed recirculation pumps (Saha, 1977).

The sixth-generation design, introduced in 1972, marked a pivotal advancement with the implementation of 8x8 fuel assembly configurations. Additional refinements

encompassed modifications to ECCS containment architecture and control rod drive systems (Halsall, 1977) (Scott, 1985).

### 2.3 Boiling Phenomenon

The boiling process represents a phase transformation where liquid converts to vapour when surrounding pressure and temperature conditions reach equilibrium. This fundamental process has commanded significant research attention due to its widespread applications. The specific case of nucleate boiling manifests when surface temperatures exceed the fluid's saturation point while maintaining heat flux below critical thresholds.

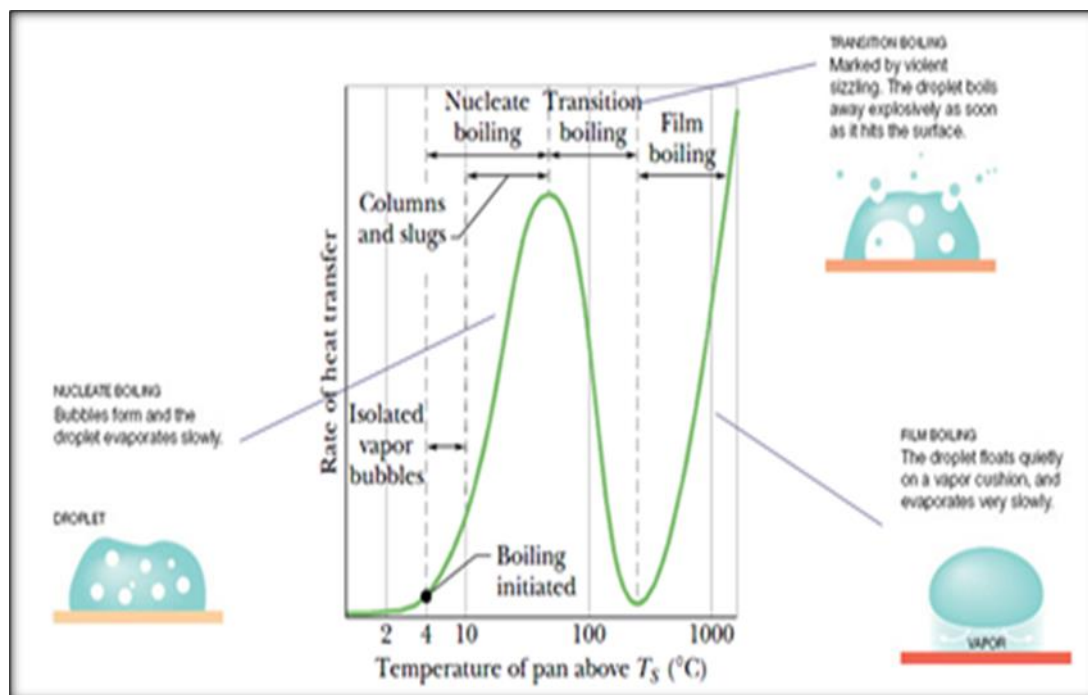


Figure 2.1: Boiling Phenomena in Water

As illustrated in Figure 2.1, water exhibits nucleate boiling characteristics when surface temperatures surpass saturation temperature ( $T_s$ ) by a differential ranging from  $10^{\circ}\text{C}$  to  $30^{\circ}\text{C}$  ( $18^{\circ}\text{F}$  to  $54^{\circ}\text{F}$ ). This regime terminates at the critical heat flux point, marking the transition to different boiling mechanisms (Sateesh & Balakrishnan, 2005).

Nukiyama's groundbreaking study from 1934 has undoubtedly guided several investigators in the understanding of boiling heat transfer mechanisms. The internal surface heat flux, the wall superheats carried out, gave rise to the boiling curve. This work also allowed him to classify the process into several boiling regimes: free convection, nucleate (with jets and columns present), intermediate, and film boiling (Thom *et al.*, 1965). He noticed that up to a certain temperature, the surface heat flux and surface temperature are dependent on each other. Above this point, the temperature could be increased with a corresponding increase in heat flux but to a lesser extent than before. The description of the upper bound of the heat flux, called the critical heat flux or CHF,

served as an important factor in predicting the failure of materials when subjected to heating (Mishima & Ishii, 1982; Ioilev *et al.*, 2007).

Thus, building on this initial framework, in 1952, Rohsenow introduced another investigation that presented some correlations between wall superheat and heat flux in the case of nucleate boiling and incorporated surface-fluid coefficients for the different materials used (Shah, 1982).

Further advances emerged through Hsu and Graham's 1961 research, which established criteria for nucleation site activation. Their findings demonstrated that active cavity size boundaries depended on multiple variables, including subcooling effects, pressure conditions, and thermal boundary layer dimensions. These insights proved particularly relevant as pool boiling heat transfer mechanisms showed strong dependence on contact line dynamics and interfacial behaviour, suggesting that microscale surface modifications could significantly influence heat transfer characteristics (Shah, 1982; Saha, 1977; Shoji, 2004).

## 2.5 Working Parameters

In the boundary layer of a nuclear reactor, there are many interesting parameters of the property of the body are determined. Thus, it is of great engineering significance in most applications. Most of the useful parameters are presented below in order to review and study the characteristics of the effective working states.

### 2.5.1 Reynolds Number

The Reynolds number ( $Re$ ) is a dimensionless quantity utilized to help predict analogous flow patterns across different fluid flow situations. George Gabriel Stokes introduced the concept in 1851. Osborne Reynolds (1842-1912) subsequently popularized the practical application of this concept in 1883, after which it was named.

The Reynolds number is defined as the ratio of inertial forces to viscous forces, quantifying the relative significance of these two force types for given flow conditions. Reynolds numbers arise when performing dimensional analysis of fluid dynamics (Wilcox, 1998).

The Reynolds number can be defined as:

$$Re = \frac{\text{Inertial force}}{\text{Viscous force}} = \frac{\rho v L}{\mu} = \frac{v L}{\nu}$$

where:

$v$  is the velocity of the object relative to the fluid,

$L$  is a characteristic linear dimension,

$\mu$  is the dynamic viscosity of the fluid ( $\text{kg}/(\text{m}\cdot\text{s})$  or  $\text{N}\cdot\text{s}/\text{m}^2$ ),

$\nu$  is the kinematic viscosity ( $\nu = \frac{\mu}{\rho}$ ) ( $\text{m}^2/\text{s}$ ), and

$\rho$  is the density of the fluid ( $\text{kg}/\text{m}^3$ ).

### 2.5.2 Prandtl Number

The Prandtl number ( $Pr$ ) is a dimensionless number, named after the German physicist Ludwig Prandtl, defined as the ratio of momentum diffusivity to thermal diffusivity. In 1905, Ludwig Prandtl introduced the concept of the boundary layer, hypothesizing that viscous effects were negligible everywhere except in a thin layer close to the solid boundary where the no-slip condition had to be fulfilled.

The Prandtl number formula is given as:

$$Pr = \frac{\text{momentum diffusivity}}{\text{thermal diffusivity}} = \frac{\nu}{\alpha} = \frac{\mu c_p}{k}$$

where:

$\nu$ : momentum diffusivity (kinematic viscosity),

$\alpha$ : thermal diffusivity,

$\mu$ : dynamic viscosity,

$k$ : thermal conductivity,

$c_p$ : specific heat, and

$\rho$ : density.

Typical values for  $Pr$  are 0.71 for air and many other gases, around 7 for water, between 100 and 40,000 for engine oil, and around 0.025 for mercury (White, 2006). The first such direct numerical simulations were performed by Rogers *et al.* in 1986, presenting the homogeneous shear flow, and by Kim and Moin in 1989, who studied channel flow for  $Pr = 0.1, 0.71$ , and 2.0. The Prandtl number also significantly impacts boundary layer interactions within the case study structure (Grasset & Parmentier, 1998).

## 2.6 Turbulence Modelling

In advancing our comprehension of convective heat transfer mechanisms and refining engineering correlations, computational approaches have emerged as invaluable analytical tools. Among these methodologies, the Reynolds-Averaged Navier-Stokes (RANS) framework stands out as a particularly effective technique for fluid behaviour analysis. The use of time-averaged parameters presents clear benefits in terms of the computational efficiency. When analyzed under simple channel configurations, boiling fluid systems allow us to use RANS turbulence modelling to represent the process in its thermodynamically steady state. The following sections address practical implementations of various RANS model variants and their relevance to the current research (Speziale, 1998).

### 2.6.1 RANS Equations

The heat transfer process of fluids under supercritical pressure is treated as a constant pressure process which is characteristic of most of the heat transfer problems found in the low-speed incompressible flow with variable density. General governing equations

necessary to predict the flow and heat transfer in supercritical fluids are presented as follows (Speziale, 1998; Bazilevs *et al.*, 2007):

### a) Continuity of Mass Equation

The continuity equation ensures the conservation of mass in the fluid flow:

$$\frac{\partial \rho}{\partial t} + \frac{\partial(\rho u_i)}{\partial x_i} = 0$$

Where

$\rho$  is fluid density,

$u_i$  represents velocity components, and

$x_i$  denotes coordinate directions.

### b) Momentum Equations

The momentum equations describe the motion of fluid particles, incorporating inertial, viscous, and pressure forces:

$$\frac{\partial(\rho u_i)}{\partial t} + \frac{\partial(\rho u_i u_j)}{\partial x_j} = -\frac{\partial p}{\partial x_i} + \frac{\partial}{\partial x_j} \left( \mu \left( \frac{\partial u_i}{\partial x_j} + \frac{\partial u_j}{\partial x_i} \right) \right) + \frac{\partial \tau_{ij}}{\partial x_j}$$

where

$p$  is pressure,

$\mu$  is dynamic viscosity, and

$\tau_{ij}$  represents the Reynolds stresses due to turbulence.

### c) Energy Equation

The energy equation accounts for heat transfer in the fluid:

$$\frac{\partial(\rho E)}{\partial t} + \frac{\partial(\rho E u_j)}{\partial x_j} = \frac{\partial}{\partial x_j} \left( k \frac{\partial T}{\partial x_j} \right) + \Phi$$

where

$E$  is the total energy per unit mass,

$k$  is the thermal conductivity,

$T$  is temperature, and

$\Phi$  represents viscous dissipation.

In these equations,  $u_i$  denotes a velocity component, and  $x_i$  represents a coordinate direction. Turbulent heat flux is modeled using eddy viscosity:

$$\text{Turbulent Heat Flux} = -\frac{\mu_t}{Pr_t} \frac{\partial T}{\partial x}$$



where

$Pr_t$  is the turbulent Prandtl number, with a default value of 0.9 in CFX, and  $\mu_t$  is the turbulent viscosity.

This approach, incorporating a molecular heat capacity  $c_p$ , is widely used in turbulence models and is considered a "standard" method.

### 2.6.2 Standard k- $\epsilon$ Model

Among turbulence modelling approaches, two-equation formulations represent the most fundamental yet comprehensive framework, wherein paired transport equations enable independent determination of turbulent velocity and length parameters. Within the FLUENT environment, the k-epsilon implementation exemplifies this category and has established itself as the cornerstone methodology for engineering fluid dynamics since its introduction by Launder and Spalding. Its widespread adoption in industrial thermal-fluid analysis stems from three key attributes: computational stability, resource efficiency, and satisfactory precision across diverse turbulent flow scenarios. The model's semi-empirical nature combines theoretical foundations with experimental validation, integrating both phenomenological insights and empirical correlations (Wilcox, 1998).

### 2.6.3 RNG k-epsilon Model

The second approach uses the RNG model. It was introduced by Yakhot *et al.* as a method that employed Re-Normalisation Group (RNG) methods to renormalise the Navier-Stokes equations for smaller scales of motion. In the conventional k-epsilon modelling, the value of eddy viscosity is calculated by assuming a single value of turbulence length scale. Thus, the turbulent diffusion calculated is only at the specified scale. However, in reality, every size of motion will contribute towards the turbulent diffusion. The same procedure, which is the RNG approach, allows for the modification of the epsilon equation suitable for turbulence modelling, which is very akin to k-epsilon modelling and aims to modify the production term due to different scales of motions in the equation (Han & Reitz, 1995).

Concerning fluid dynamics, recent improvements in turbulence modelling, especially Large Eddy Simulation (LES) and Direct Numerical Simulation (DNS), are useful for the analysis of complex flows associated with nuclear reactors. These models produce high-quality simulations by resolving the smaller turbulence structures more accurately. The above-mentioned LES and DNS methods, however, possess a high computational burden that often involves enormous costs. Therefore, their useful implementation in very large systems such as nuclear power stations is often limited. On the other hand, the Reynolds-Averaged Navier-Stokes (RANS) model is less detailed yet computationally inexpensive and, therefore, practical for industrial use. RANS is thus suitable for this investigation as it models boiling water flow within the time and resource constraints. Thus, this decision provides a reasonable but powerful way to model cooling flow in a nuclear reactor, which is consistent with the operation of actual reactor management.

### 3. Methodology

#### 3.1 Introduction

This study aims to devise a numerical model to predict the heat transfer characteristics along the modelled channel so that the boiling behaviour of water under the condition of circulated water in a nuclear reactor can be investigated. The computations included were for heat and fluid flow, which required CFD for the simulation of fluids interacting with different effective properties and initial conditions.

The methodological procedure of this research will apply the tested model by applying the concept of discretisation of the partial differential equations to a given finite number of control volumes, which are called meshes and cells. The next step will be for the solver to formulate the general governing equations for mass, momentum and energy. The partial differential equations are solved numerically to render the solution field based on CFD Analysis. ANSYS can be implemented in the CFD model, along with the unique experimental data and the assumptions, such as dimensions and the specified values for flow and temperature.

#### 3.2 Modelling Implementation

The commercial software used to solve CFD problems can be expressed by FLUENT. They represent the base of the ANSYS 16.2 simulation program and are employed in the current study as a general modelling process following the same procedure. The CFD modelling sequence could be classified into a few major steps:

The pre-processing stage, models step and solving, followed by the post-processing stage. This step will contain the tasks of preparing the geometrical shape of the experiment, which is constructed for mesh generation. It is then followed by fixing the physical model, boundary conditions, initial conditions, and other appropriate parameters that were defined in the model step and solving. The obtained results throughout the computational domain will be presented in the post-processing stage.

The execution of the CFD simulations was not without its drawbacks as regards defining the boundary conditions and choosing the initial parameters. Variation of certain fluid properties like viscosity and density at higher temperatures was thus assumed to modify the model. Also, while generating the mesh, there was a need to strike a balance between fine mesh and computational resources to achieve reliable results without wasting available resources. The accuracy of the turbulence models and boundary layers was investigated through the preliminary tests, whereby mesh sizes that were efficient in simulating the processes that were taking place were found. Although these changes were not substantial mitigations, they however made it possible to develop a compromise simulation setup with the most vital aspects taken into consideration, thus increasing the usability of the model.

### 3.3 Initial Study

The initial study represents the basis for the optimization or the evaluation process. During each iteration, the program runs these studies with modified variables. The requirements for initial studies depend on the constraints and goals of the study.

The first role in the initial study is that all studies referenced in defining constraints and goals must belong to the same configuration. The phases considered below:

#### 3.3.1 The First Phase: Using the SolidWork program

SolidWorks mechanical design automation software is a feature-based, parametric solid modelling design tool that takes advantage of the easy-to-use graphical user interface. The steps to create the geometrical shape are as follows:

- **Step 1:** Creating the model and dimensioning it.  
After starting the program, we will choose the correct plane to sketch on. This is accomplished by selecting the best profile to sketch the part. The best profile to sketch is the one which, when extruded, generates the majority or most complexities of the part. The direction we look at the part to get the best profile - whether it is the plan, elevation or end view - will determine sketching on the Top, Front or Right Plane. By giving careful thought to which plane is used to sketch the profile, the proper views are easily generated on the detailed drawing.
- **Step 2:** Convert the geometrical drawing to the IGS extension file.

#### 3.3.2 The Second Phase: Using the ANSYS Program

Computational fluid dynamics, usually abbreviated as CFD, utilizes numerical methods and algorithms to solve and analyze problems involving fluid flows. Computers are employed to perform the calculations required to simulate the interaction of liquids and gases with surfaces defined by boundary conditions. With high-speed supercomputers, better solutions can be achieved. Ongoing research yields software that enhances the accuracy and speed of complex simulation scenarios such as transonic or turbulent flows. The independent software to be used will be the ANSYS program. In order to prepare for the use of the ANSYS software, a new Fluent fluid flow analysis system must be created by double-clicking the Fluid Flow (Fluent) option under Analysis Systems in the Toolbox. The fluid flow analysis system consists of various cells (Geometry, Mesh, etc.) that represent the workflow for performing the analysis. ANSYS Workbench is composed of multiple data-integrated and native applications in a single, seamless project flow, where individual cells can obtain data from other cells and provide data to other cells.

- **Step 1:** Creating the Geometry

In order to create geometry in ANSYS software, an import code is used to transfer the appropriate geometry file. In this step, the drawn shape geometry is created in ANSYS DesignModeler using Import Geometry code, and then the list of Fluent files is updated in ANSYS Workbench.

- **Step 2: Meshing the Geometry**

The computational domain undergoes discretization into numerous finite elements, a procedure known as mesh generation, resulting in a discrete grid structure. This discretization framework enables detailed analysis of flow parameters - including pressure distributions and velocity fields - at individual element locations.

Implementation requires generating a comprehensive computational grid throughout the solution domain utilizing ANSYS Meshing functionality for CFD analysis preparation. Grid resolution directly correlates with analytical precision, as increased element density provides enhanced sampling points for parameter evaluation. In two-dimensional applications, mesh construction employs either triangular or quadrilateral elements, each yielding distinct grid characteristics: triangular configurations produce unstructured arrangements, while quadrilateral elements generate structured grid patterns. Mesh definition proceeds through the specification of either total element quantity or individual element dimensions. Edge size control functionality enables precise manipulation of element dimensions along geometric boundaries, surfaces, and volumetric regions. For this analysis, we implement a uniform structured grid with 0.02m spacing.

- **Step 3: Setting Up the CFD Simulation in ANSYS Fluent.**

After creating a computational mesh for the selected geometry, this step will set up a CFD analysis using ANSYS Fluent, and then review the list of files generated by ANSYS Workbench. The procedure of this work is as follows:

- a) **Start ANSYS Fluent**

In the ANSYS Workbench Project Schematic, The Fluent Launcher allows the start up ANSYS Fluent based on the pre-processed geometry.

- b) **Set general settings for the CFD analysis**

In order to solve the case study problems, a general code will be selected in the navigation pane to perform the mesh-related activities and to choose a solver. In this step, the shape working conditions must be fixed in order to specify the right dimensions and flow direction.

- a) Change the units for length.

- i. Select length in the Quantities list.
- ii. Select mm in the Units list.
- iii. Close the dialog box.

- b) Check the mesh.

- c) Specify the water flow gravity.

ANSYS Fluent will report the results of the mesh check in the console.

- **Step 4: Set up models for the CFD simulation**

In this step, the model will be specified. It is an important part of the simulation procedure because the accuracy of the results depends on the model type. For this reason, the present procedure must be done as follows:

- a) Select Models code.
- b) Enable heat transfer by activating the energy equation.
  - i. Enable the Energy Equation option.
  - ii. Click OK to close the Energy dialogue box.
- c) Enable the k- $\epsilon$  turbulence model.
  - i. Use the best (by trial) k-epsilon Model list.
  - ii. Select the Near-Wall Treatment.

- **Step 5:** Set up materials for the CFD simulation

This step will provide the name and specification of each part as in the procedure:

- a) Create a new material called water using the Create/Edit Materials dialogue box.
  - i. Type of water (liquid, vapour),
  - ii. Specify the characteristic by (Change/Create).
- b) Create a new material for the heater rod part
  - i. Type of material (steel, copper),
  - ii. Specify the characteristic by (Change/Create).

- **Step 6:** Set up the boundary conditions for the CFD analysis

- a) Specify the Velocity

It has already been tried and tested in the field of water flow in nuclear reactors. The FLUENT software solves the 3-D Reynolds-Navier-Stokes equations for the mass-averaged velocity, time-averaged pressure, energy and density. The software is an integrated and complex Navier-Stokes fluid flow prediction system, capable of diverse and complex multi-dimensional fluid flow problems. It utilizes a flexible, multi-block grid system, a graphical interface and several sophisticated modelling tools, making it suitable for water flow simulation. The fluid flow solver, FLUENT, provides solutions for incompressible/compressible, steady-state/transient, laminar/turbulent single-phase fluid flow in complex geometries. To specify the water details, the following steps must be done:

- i. Enter y-velocity,
- ii. Specify the flow direction,
- iii. Specify the water temperature.

- **Step 7:** Set up the solution Initialization

This step is an essential step in calculating the simulation variables. The procedure in this step prepares the data which will be used in the run step. The procedure to select in this step is as follows:

- a) Click solution Initialization,
- b) Select standard Initialization,
- c) Choose from the code (compute from) the calculation starting,
- d) Check from initial values slid all the working values,
- e) Initialize the data.

### **Step 8: Calculate a solution**

Running the solver is an important phase in the ANSYS system. It is a powerful tool to describe the heat transfer behaviour, and the continuity, momentum, and energy equations are required. The essential points in this step are the date of working variables and the number of iterations.

### **3.4 Post-processing**

The run results can be expressed as data carried out using the ANSYS software analyser. The primary objective of this study is to focus on the water flow distribution inside the channel and investigate the boiling water phenomenon. The vectors of water velocity and temperatures will be plotted along with a few remarks and observations about the simulation. Post-processing tools (XY plot or contour plot) are used to check the grid placement and the solution profile.

### **3.5 Solution Strategy**

Any transient solution of numerical modelling needs an approaching strategy. This strategy can be set up based on the limitations of the numerical models or the physics of the real operating conditions. All these approaches may affect the calculation convergences, simulation results, and numerical computational times. Three different cases can be employed in this study:

- **First Case:** The water velocity is set to 0.45 m/s, with five different temperatures applied in this case: 100°C, 200°C, 300°C, 400°C, and 500°C.
- **Second Case:** The water velocity is set to 0.89 m/s, with the same five temperature settings: 100°C, 200°C, 300°C, 400°C, and 500°C.
- **Third Case:** The water velocity is set to 1.34 m/s, also using five temperature settings: 100°C, 200°C, 300°C, 400°C, and 500°C.

## **4. Results and Discussion**

### **4.1 Verification and Validation**

Due to the necessity of modeling the boiling water flow in different cases, it is necessary to consider the accuracy of the CFD method with the aid of experimental data. The validation test is a method to minimize and quantify modelling errors, ensuring that the CFD model being solved is a good representation of reality. To examine the effect of the variation of any particular parameter in the simulation, the sensitivity study is the first to be performed before the validation. This study conducted sensitivity analyses on node numbers, grid types, and turbulence models.

#### **4.1.1 Experimental Results**

In this section, the experimental results were performed by applying heat flux to different mass flows of water.

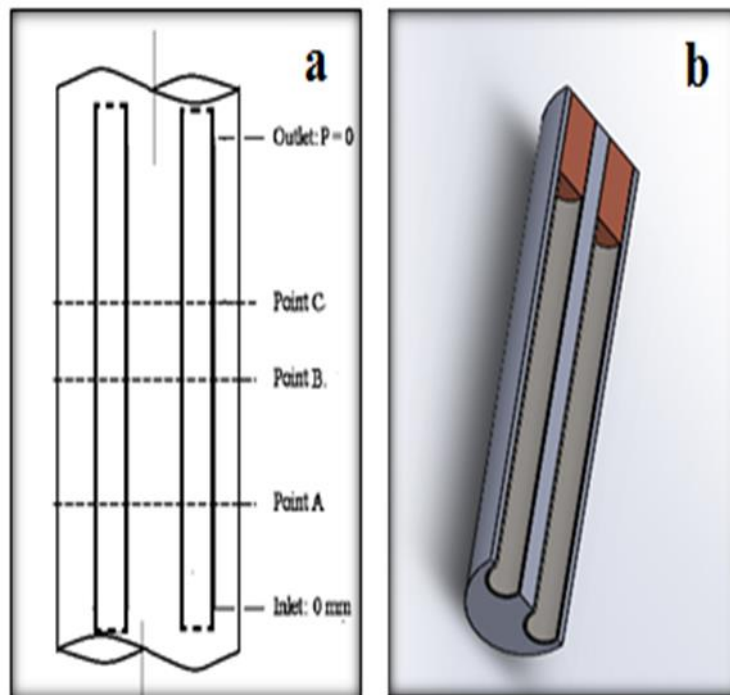


**Figure 4.1:** Experimental Channel, a) Schematic Diagram, b) Solid Work Sample

A schematic diagram of the experimental channel domain is shown in Figure 4.1. The computational domain can be considered as a three-dimensional region. The model describes a turbulent flow with a channel diameter of 30 mm and a length of 3000 mm involving water flow cases. The heat flux ( $q$ ) is imposed on the inner side of the computational domain, and the adiabatic boundary condition is used for the outer wall. The heat roads' position in the channel is longitudinal with a diameter of 10mm; additionally, the fluid flows upward in the channel around the two heat source roads.

#### 4.1.2 Turbulence Model Study

Turbulence Model study is used to qualify the differences in temperature distribution effect along the circular channel. The essential issue for a good performance of the model is the chosen model type. In this study, three turbulence models are employed to predict the flow behaviour in the considered physical domain, which are The Renormalization Group (RNG), Reynolds stress models (RSM) and realizable k-epsilon model (RKE).

The reason for the realizable k- $\epsilon$  model (RKE) success contains a new formulation for the turbulent viscosity and a new transport equation for the dissipation rate,  $\epsilon$ , that is derived from an exact equation for the transport of the mean-square vorticity fluctuation. Also, it provides superior performance for flows involving rotation and boundary layers under strong adverse pressure gradients, separation, and recirculation.

## 4.2 Velocity Profiles

The effect of different water velocities represents a key parameter that affects the overall mass transfer. The results of the simulation scenario show the water velocity behaviour. This behaviour indicates that the water velocity increases along the channel distance in certain places and decreases in other places along the channel. That is clear from the red colour as an indicator in the simulation section images. The reason for that is the decrease in the flow area. The friction with the outer surfaces, in addition to the narrow pass between the channel and the road, causes a reduction in the water flow. It is clear from the blue colour In the simulation Images that there Is a high flow reduction In this area, which narrows the channel area and causes a clear increase in the water velocity in the middle of the channel.

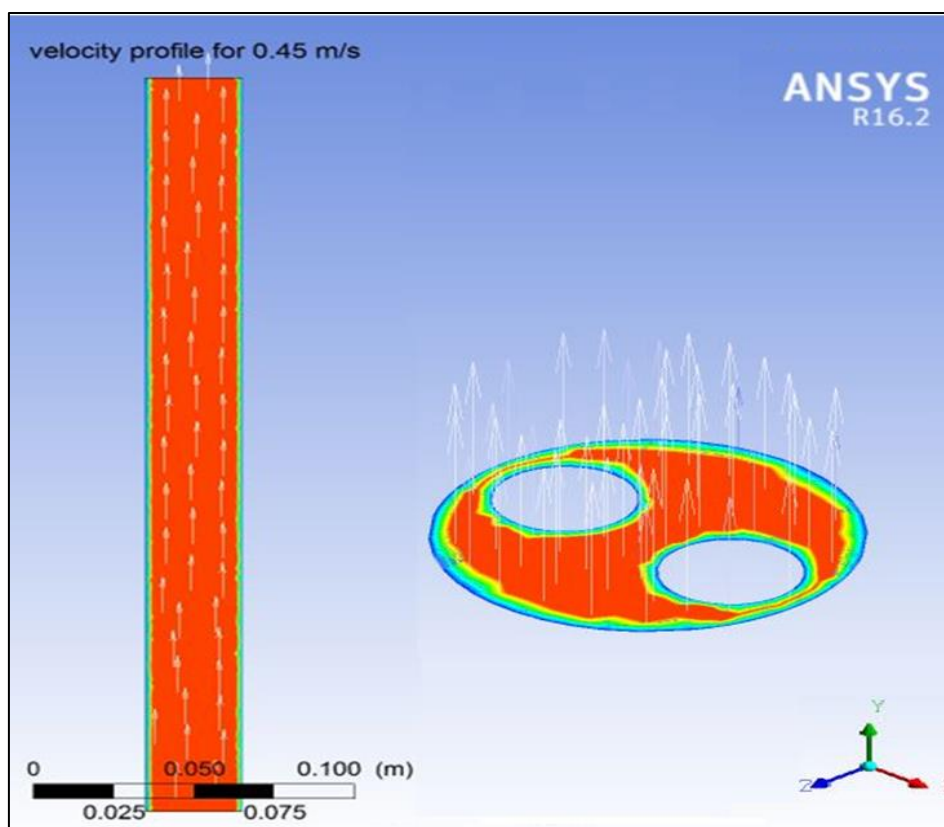


Figure 5.3: Streamlines of the Water Flow in the Channel

Streamlines in the channel flow are exhibited in Figure 5.3. A typical flow pattern is observed, which moves upward along the tube, especially in the centre. Thus, a vortex symmetric about the vertical centre line is formed. This point will be useful in considering the heat change measurement in the next section. The stable water movement will observe an independent heat change along the channel.

Three cases of water velocity have been used in the simulation tests. The first is 0.45 m/s, the second is 0.89 m/s, and the third is 1.34 m/s. The phenomenon presented was observed in the same way in the three cases.



### 4.3 Temperature Profiles

The resulting temperature distribution is shown in Figures 5.4 to 5.6. The contour shows the temperature profile along the channel on both sides of the heat roads. At the same time, the contour shows the temperature distribution at the x-z plane. It can be observed that there are three main regions in the temperature distribution: the first is the higher temperature, which occurs beside the heater wall, and the second is the hot water area, which covers most of the water flow area in aqua colour. The third area is the cold area in blue colour which represents the faraway regions.

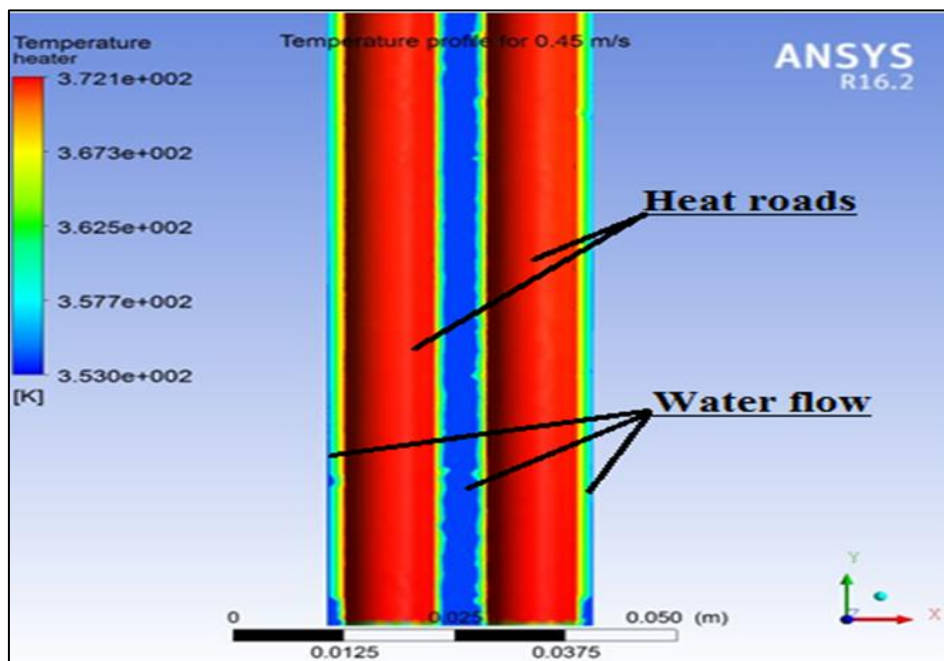


Figure 5.4: General Heat Roads with the Boundary of the Experiment

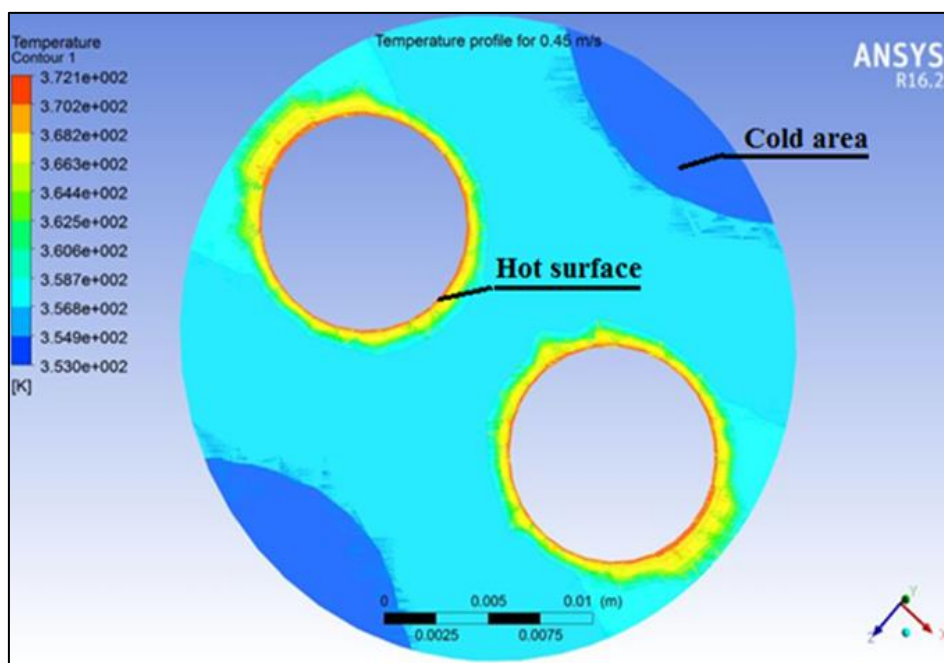


Figure 5.5: Section of Water Regions

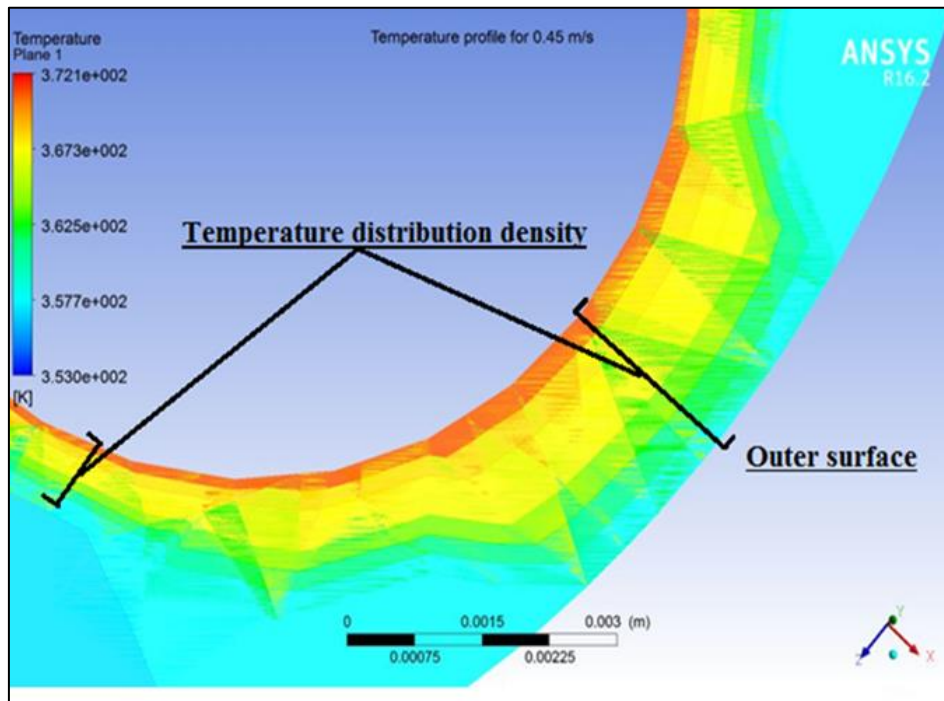


Figure 5.6: Heat Distribution around the Heat Road

The temperature decreases far away from the heat road surface. The temperature distribution at the planes between the heat road and the outer surface shows that the temperature distribution in this area is higher near the heat road, and the diffusion of heat is greater toward the outer wall of the channel.

The heat density toward the outer wall is high and diffusive. It's because of the low velocity in this area, as presented in section 4.2.

The fluid motion in the y-direction can vary due to the x-y plane and x-z plan. To be sure that the simulation scenario can observe the nearest indicator to the actual situation. The temperature values have been measured in different positions and at different channel levels. The temperature was measured in different places along the channel, and many situations were observed.

The first situation is the constant temperature in the distance 13mm and 3 mm, which represents the heater surface. The temperature in this region is constant because it represents the heart wall temperature. The other two regions are the temperature in the centre of the channel and the temperature in the outer surface. It is clear from the high increase of the temperature value at a distance of 15mm that the outer surface of the channel contains a high ability to heat the water. That is because of the low velocity, as mentioned before.

#### 4.3.1 Temperature Profile of the First Case

The first case of study is water velocity at 0.45 m/s in (-y) centre point direction of the channel. It is noted that temperature growth happens at all measured points. The highest water temperature is 500 °C, and its magnitude is about 409 °K (135.85 °C). This observation can be used as an important point of possibility to reach the saturated

temperature of water in the shortest time. It also indicates that the vapour at this temperature can be superheated and eliminate the wet percentage in the vapour, which makes the vapour more effective in injecting in the turbines.

#### **4.3.2 Temperature Profile of the Second Case**

The second case of study is water velocity at 0.98 m/s in (-y) centre point direction of the channel. It is noted that the temperature growth happened in all measured points at 0.45 m/s. The highest water temperature is 500 °C, and its magnitude is about 413.5 °K (140.35 °C). This behaviour is similar to the results observed in 0.45 m/s, which is possible to reach the water temperature into the saturated point of water degree in the shortest time. Also it can indicate that the vapour in this temperature can be superheated and eliminate the wet percentage in the vapour and that make the vapour more effective in injecting in the turbines.

#### **4.3.3 Temperature Profile of the Third Case**

The third case of study is water velocity at 1.34 m/s in (-y) centre point direction of the channel. Also, it is noted that the temperature growth happened in all measured points as in the 0.45 m/s and 0.89 m/s. The highest water temperature is 500 °C, and its magnitude is about 419.4 °K (146.25 °C). This behaviour is similar to the results observed in 0.45 m/s and 0.89 m/s, which is also useful to reach the water temperature into the saturated point of water degree in the shortest time, and it can be superheated and eliminate the wet percentage in the vapour and that make the vapour more effective in injecting in the turbines.

#### **4.3.4 Temperature Behaviour**

To understand the differences between the three cases, the changes in water temperature with respect to different distances in the channel longitudinal regions using the centre of the channel as a reference to take all the values were analysed.

The water temperature is taken as a bulk temperature. The plots can observe the temperature growth behaviour in order to investigate the different regions, correlated with different source temperature relationships.

The water temperature degrees were decreased with the rise of water velocity, but with the increase of heat road temperature over 200 °C, the water temperature increased in the range of 200 °C to 500 °C. This phenomenon can describe the behaviour of heat transfer based on different resource temperatures with respect to different water velocities. This information is useful in the design phase, as it can present a practical view of designing the capacity of water pumps and pipe sizes of the nuclear system. Also, the water flow behaviour to the difference in source temperature can help to specify the water flow control dimensions to determine the water circulation quantity to invest in the nucleate heat source.

#### 4.4 Heat Flux Profiles

The model is tested compared to three cases for the channel flow with the same regular changes. The experimental data is at a heat flux and observes a low value for low velocity. The linear increase in heat flux indicates the fully developed condition. The thermal boundary layer is identified due to high heat flux, and the heat distribution is almost uniform along the channel. It is also observed that the significant flow with the suitable amount of heat flux is 0.89 m/s because the amount of heat flux became more than the 0.45 m/s flow velocity, which rose by about 61%. Nevertheless, it does not arise when the velocity becomes 1.34 m/s. It decreases by about 2%. That indicates a stronger natural convection in the flow of 0.89 m/s, which can represent a good solution for the dry-out problem which represents the major problem in BWR systems.

#### 5. Conclusions

The objective of this research is to investigate the effects of heat transfer from the nuclear heat source to the moving water through the longitudinal direction of the source. Experiments were conducted on the electrical heat source with varying heat flux to evaluate the heat convection through the water and investigate the properties of heated water correlated with the boiling point. Then the experiments were simulated by ANSYS CFD code, FLUENT to analyse the boiling water phenomenon deeply. This method was validated by running a few case studies.

- 1) It is observed from the result that the calculation showed the difference in the maximum and the minimum flow rates in the channel section is only 3.11 %; therefore, it was concluded that there is no significant distribution of the heat in the section of the channel. The present result is based on the difference in water flow velocity in the section. The friction loss in the area between the heat road and the outer surface reduces the water flow velocity. With the low velocity the heat defused will arise in quick form.
- 2) There is a clear relationship between the water temperature and the heat road temperature. When the heat road increases the water temperature increases also. The amount of water temperature increases reached 13% in flow of 0.45 m/s. In the water flow velocity of 0.89 m/s, the temperature percentage increases to 16.3%. While in the flow of 1.34 m/s, the results observed a 17% increase in water temperature. In general, these results indicate that there is a limitation to the water temperature increase based on the water velocity. It's also clear that the time of temperature rise was short a velocity of 1.34 m/s compared with the other two velocities.
- 3) The other observation in this study is the alternate water temperature due to certain temperatures. It is clear from the results that when the water velocity increases, the water temperature degrees decrease. This behaviour appears below the 200°C of the heat road. But over this degree, the water temperature increases.

- 4) The last observation in this study can describe the heat flux changes along the channel. The rate of heat flux in the system was 6736.557 W/1°C for each square meter of heat generation. This fact is useful in calculating the time needed to reach the boiling point in the reactor.
- 5) From the model tests, the results observed that the best model was RKE due to its ability to calculate the effect of the circle shape of heat distribution.
- 6) CFD was a significant program in the research due to its low cost compared with the cost of laboratory experiments.

### **5.1 Reflection on Simulation Accuracy and Practicality**

The CFD modelling in this work has driven home the practicality of using simulation capability in the study of complex heat transfer phenomena within a nuclear reactor. While laboratory experiments are invaluable, CFD provides the added flexibility to vary parameters and conditions using cost-effective controlled virtual environments. It also allows for the detailed consideration of variables like water flow, temperature gradients, and turbulence models- all without the extreme costs and risks associated with physical reactor testing. Therefore, the CFD results provided herein confirm experimental findings and show the feasibility of simulation applied complementarily for reactor design and safety evaluations.

### **5.2 Implications for Reactor Efficiency and Safety**

These results show that water velocity optimization can have considerable consequences on the efficiency of a heat transfer process in reactor cooling systems and hence plays a vital role in reactor safety improvement. More precisely, the most favourable compromise between heat removal and coolant stability was reached at 0.89 m/s velocity. This important conclusion is drawn from this outcome for the operators of reactors while mitigating risks of localized overheating and dry-out phenomena.

Correspondingly, such findings could realize the recommended operational settings that may actually enable extending the service life of reactors and sustaining a uniform energy output while even reducing maintenance costs by lessening the thermal stresses among components.

### **5.3 Broader Impact on Nuclear Reactor Design**

The conclusions on coolant flow rate versus heat flux and temperature distribution obtained in this study provide practical guidelines for reactor engineers and designers. It is possible to develop reactors that have the greatest amount of stability for high-power conditions by integrating such parameters during the design phase, thus assuring more reliable energy output. Such findings would also provide the necessary background for modification in existing reactors, allowing retrofitting options to bring more efficiency and safety to the current cooling systems. To this understanding, this research will fit well into the ongoing effort in the nuclear industry to optimize reactor performance and

limit chances of risk, proving relevance to new designs as well as operational improvement of existing reactors.

#### 5.4 Future Directions for Model Development and Validation

Further refinement may consider transient flow conditions, more advanced models of turbulence, and multi-phase flow analysis to enhance the predictive capabilities of CFD models. A higher degree of refinement in a model would yield higher accuracy in determining the location of critical heat flux and failure zones at different operating conditions. This would probably put CFD among those very useful tools in nuclear reactor research to help evolve much safer and more efficient nuclear power systems. Future further studies may be directed to the application of machine learning algorithms in an attempt to optimize the choice of simulation parameters with the aim of computational cost reduction and increasing the accuracy of the results.

#### Conflict of Interest Statement

The authors declare no conflicts of interest.

#### About the Author(s)

**Magdi Saad Farag Ali** is a lecturer at Higher Institute of Science and Technology Ajdabiya, Libya and Head of the Petroleum Engineering Department.

**Hani Saed Faraj Ali** is a PhD Candidate.

#### References

- Amselem Abecasis, E. (2010). *Analysis of boiling water reactor design and operating conditions effect on stability behaviour*. Retrieved from [https://www.researchgate.net/publication/278002329\\_Analysis\\_of\\_Boiling\\_Water\\_Reactor\\_Design\\_and\\_Operating\\_Conditions\\_Effect\\_on\\_Stability\\_Behaviour](https://www.researchgate.net/publication/278002329_Analysis_of_Boiling_Water_Reactor_Design_and_Operating_Conditions_Effect_on_Stability_Behaviour)
- Basu, N., Warriar, G. R., & Dhir, V. K. (2005). Wall heat flux partitioning during subcooled flow boiling: Part 1—Model development. *Journal of Heat Transfer*, 127(2), 131-140. <https://doi.org/10.1115/1.1842784>
- Bazilevs, Y., Calo, V. M., Cottrell, J. A., Hughes, T. J. R., Reali, A., & Scovazzi, G. (2007). Variational multiscale residual-based turbulence modeling for large eddy simulation of incompressible flows. *Computer Methods in Applied Mechanics and Engineering*, 197(1), 173-201. Retrieved from <https://www.odn.utexas.edu/media/reports/2007/0715.pdf>
- Board, A. E. R. (2002). *Annual report 2001-2002*. Atomic Energy Regulatory Board.
- Bonjour, J., & Lallemand, M. (1998). Flow patterns during boiling in a narrow space between two vertical surfaces. *International Journal of Multiphase Flow*, 24(6), 947-960.

[https://ui.adsabs.harvard.edu/link\\_gateway/1998IJMF...24..947B/doi:10.1016/S0301-9322\(98\)00017-2](https://ui.adsabs.harvard.edu/link_gateway/1998IJMF...24..947B/doi:10.1016/S0301-9322(98)00017-2)

- Buongiorno, J., Hu, L. W., Apostolakis, G., Hannink, R., Lucas, T., & Chupin, A. (2009). A feasibility assessment of the use of nanofluids to enhance the in-vessel retention capability in light-water reactors. *Nuclear Engineering and Design*, 239(5), 941-948. Retrieved from <http://dx.doi.org/10.1016/j.nucengdes.2008.06.017>
- Dokhane, A. (2004). *BWR stability and bifurcation analysis using a novel reduced order model and the system code RAMONA* (Doctoral dissertation, École Polytechnique Fédérale de Lausanne). Retrieved from <http://dx.doi.org/10.5075/epfl-thesis-2927>
- Graham, J. (Ed.). (2012). *Fast reactor safety*. Elsevier. Retrieved from [https://books.google.ro/books/about/Fast\\_Reactor\\_Safety.html?id=A8p4AAAIAAJ&redir\\_esc=y](https://books.google.ro/books/about/Fast_Reactor_Safety.html?id=A8p4AAAIAAJ&redir_esc=y)
- Grasset, O., & Parmentier, E. M. (1998). Thermal convection in a volumetrically heated, infinite Prandtl number fluid with strongly temperature-dependent viscosity: Implications for planetary thermal evolution. *Journal of Geophysical Research: Solid Earth*, 103(B8), 18171-18181. Retrieved from [https://agupubs.onlinelibrary.wiley.com/doi/abs/10.1029/98JB01492?utm\\_campaign=R3MR425&utm\\_content=EarthSpaceEnvirSci&utm\\_medium=paidsearch](https://agupubs.onlinelibrary.wiley.com/doi/abs/10.1029/98JB01492?utm_campaign=R3MR425&utm_content=EarthSpaceEnvirSci&utm_medium=paidsearch)
- Halsall, M. J. (1977). Review of international solutions to NEACRP benchmark BWR lattice cell problems. UKAEA.
- Han, Z., & Reitz, R. D. (1995). Turbulence modeling of internal combustion engines using RNG  $\kappa$ - $\epsilon$  models. *Combustion Science and Technology*, 106(4-6), 267-295. Retrieved from <https://doi.org/10.1080/00102209508907782>
- Ioilev, A., Samigulin, M., Ustinenko, V., Kucherova, P., Tentner, A., Lo, S., & Splawski, A. (2007). Advances in the modeling of cladding heat transfer and critical heat flux in boiling water reactor fuel assemblies. *Proc. 12th International Topical Meeting on Nuclear Reactor Thermal Hydraulics (NURETH-12)*, Pittsburgh, Pennsylvania, USA. Retrieved from [https://www.researchgate.net/publication/289080649\\_Advances\\_in\\_the\\_modeling\\_of\\_cladding\\_heat\\_transfer\\_and\\_critical\\_heat\\_flux\\_in\\_boiling\\_water\\_reactor\\_fuel\\_assemblies](https://www.researchgate.net/publication/289080649_Advances_in_the_modeling_of_cladding_heat_transfer_and_critical_heat_flux_in_boiling_water_reactor_fuel_assemblies)
- Jens, W. H., & Lottes, P. A. (1951). *Analysis of heat transfer, burnout, pressure drop and density data for high-pressure water* (No. ANL-4627). Argonne National Lab. Retrieved from <https://digital.library.unt.edu/ark:/67531/metadc1015865/>
- Kataoka, Y., Fukui, T., Hatamiya, S., Nakao, T., Naitoh, M., & Sumida, I. (1992). Experiments on convection heat transfer along a vertical flat plate between pools with different temperatures. *Nuclear Technology*, 99(3), 386-396. Retrieved from <https://doi.org/10.13182/NT92-A34722>
- Mishima, K., & Ishii, M. (1982). Critical heat-flux experiments under low-flow conditions in a vertical annulus. *NUREG/CR-2647; ANL-82-6*, Argonne National Lab. Retrieved from [https://inis.iaea.org/search/search.aspx?orig\\_q=RN:14724099](https://inis.iaea.org/search/search.aspx?orig_q=RN:14724099)

- Rainey, K. N., & You, S. M. (2001). Effects of heater size and orientation on pool boiling heat transfer from microporous coated surfaces. *International Journal of Heat and Mass Transfer*, 44(14), 2589-2599. [http://dx.doi.org/10.1016/S0017-9310\(00\)00318-5](http://dx.doi.org/10.1016/S0017-9310(00)00318-5)
- Saha, P. (1977). Review of two-phase steam-water critical flow models with emphasis on thermal non-equilibrium. *Brookhaven National Lab.* <https://www.nrc.gov/docs/ML1925/ML19256F779.pdf>
- Sanna, A., Hutter, C., Lin, H., Sefiane, K., Walton, A. J., Pavlovic, E., ... & Kenning, D. B. R. (2008). Simulation and experimental investigation of pool boiling on a silicon wafer with artificial nucleation sites. Retrieved from [https://www.researchgate.net/publication/49401709\\_Simulation\\_and\\_experimental\\_investigation\\_of\\_pool\\_boiling\\_on\\_a\\_silicon\\_wafer\\_with\\_artificial\\_nucleation\\_sites](https://www.researchgate.net/publication/49401709_Simulation_and_experimental_investigation_of_pool_boiling_on_a_silicon_wafer_with_artificial_nucleation_sites)
- Sateesh, G., Das, S. K., & Balakrishnan, A. R. (2005). Analysis of pool boiling heat transfer: Effect of bubbles sliding on the heating surface. *International Journal of Heat and Mass Transfer*, 48(8), 1543-1553. Retrieved from <http://dx.doi.org/10.1016/j.ijheatmasstransfer.2004.10.033>
- Scott, P. M. (1985). A review of environment-sensitive fracture in water reactor materials. *Corrosion Science*, 25(8), 583-606. Retrieved from <https://inis.iaea.org/collection/NCLCollectionStore/Public/17/067/17067742.pdf>
- Shah, M. M. (1976). A new correlation for heat transfer during boiling flow through pipes. *ASHRAE Transactions*, 82, 66-86. Retrieved from <https://mmshah.org/publications/CHART%20GRAPHICAL%201976.pdf>
- Shah, M. M. (1977). A general correlation for heat transfer during subcooled boiling in pipes and annuli. *ASHRAE Transactions*, 83, 205-215. Retrieved from [https://www.researchgate.net/publication/282578410\\_A\\_general\\_correlation\\_for\\_heat\\_transfer\\_during\\_subcooled\\_boiling\\_in\\_pipes\\_and\\_annuli](https://www.researchgate.net/publication/282578410_A_general_correlation_for_heat_transfer_during_subcooled_boiling_in_pipes_and_annuli)
- Shah, M. M. (1982). Chart correlation for saturated boiling heat transfer: Equations and further study. *ASHRAE Transactions*, 88, 185-196. Retrieved from [https://www.researchgate.net/publication/236520034\\_Chart\\_correlation\\_for\\_saturated\\_boiling\\_heat\\_transfer\\_Equations\\_and\\_further\\_study](https://www.researchgate.net/publication/236520034_Chart_correlation_for_saturated_boiling_heat_transfer_Equations_and_further_study)
- Shih, T. H., Zhu, J., & Lumley, J. L. (1993). A realizable Reynolds stress algebraic equation model. Retrieved from <https://ntrs.nasa.gov/citations/19930007407>
- Shoji, M. (2004). Studies of boiling chaos: A review. *International Journal of Heat and Mass Transfer*, 47, 1105-1128. Retrieved from <http://dx.doi.org/10.1016/j.ijheatmasstransfer.2003.09.024>
- Speziale, C. (1998). Turbulence modeling for time-dependent RANS and VLES: A review. *AIAA Journal*, 36(2), 173-184. Retrieved from <https://www.newsmth.net/bbsanc.php?path=/groups/sci.faq/Mechanics/Sources/Books/Papers/paper/M.1191642556.V0&ap=440>
- Steiner, H., Kobor, A., & Gebhard, L. (2005). A wall heat transfer model for subcooled boiling flow. *International Journal of Heat and Mass Transfer*, 48(19), 4161-4173.



- Retrieved from [https://online.tugraz.at/tug\\_online/voe\\_main2.getvolltext?pCurrPk=26709](https://online.tugraz.at/tug_online/voe_main2.getvolltext?pCurrPk=26709)
- Thom, J. R. S., Walker, W. M., Fallon, T. A., & Reising, G. F. S. (1965). Boiling in subcooled water during flow up heated tubes or annuli. *Proceedings of the Symposium on Boiling Heat Transfer in Steam Generating Units and Heat Exchanger*. Inst. Mech. Engrs., Manchester, England. Retrieved from [https://doi.org/10.1243/PIME\\_CONF\\_1965\\_180\\_117\\_02](https://doi.org/10.1243/PIME_CONF_1965_180_117_02)
- Thorncroft, G. E., & Klausner, J. F. (1999). The influence of vapor bubble sliding on forced convection boiling heat transfer. *Journal of Heat Transfer*, 121, 73-79. Retrieved from [https://www.researchgate.net/profile/James-Klausner/publication/245361691\\_The\\_Influence\\_of\\_Vapor\\_Bubble\\_Sliding\\_on\\_Forced\\_Convection\\_Boiling\\_Heat\\_Transfer/links/549db9420cf2b803713a7bb3/The-Influence-of-Vapor-Bubble-Sliding-on-Forced-Convection-Boiling-Heat-Transfer.pdf](https://www.researchgate.net/profile/James-Klausner/publication/245361691_The_Influence_of_Vapor_Bubble_Sliding_on_Forced_Convection_Boiling_Heat_Transfer/links/549db9420cf2b803713a7bb3/The-Influence-of-Vapor-Bubble-Sliding-on-Forced-Convection-Boiling-Heat-Transfer.pdf)
- Wilcox, D. C. (1998). *Turbulence modeling for CFD* (Vol. 2, pp. 103-217). DCW Industries. Retrieved from [https://cfd.spbstu.ru/agarbaruk/doc/2006\\_Wilcox\\_Turbulence-modeling-for-CFD.pdf](https://cfd.spbstu.ru/agarbaruk/doc/2006_Wilcox_Turbulence-modeling-for-CFD.pdf)
- Yamamoto, T., Mitachi, K., & Suzuki, T. (2005). Steady-state analysis of small molten salt reactor: Effect of fuel salt flow on reactor characteristics. *JSME International Journal Series B*, 48(3), 610-617. Retrieved from [https://www.jstage.jst.go.jp/article/jsmeb/48/3/48\\_3\\_610/\\_pdf](https://www.jstage.jst.go.jp/article/jsmeb/48/3/48_3_610/_pdf)
- Zhang, L., & Shoji, M. (2003). Nucleation site interaction in pool boiling on the artificial surface. *International Journal of Heat and Mass Transfer*, 46(3), 513-522. [http://dx.doi.org/10.1016/S0017-9310\(02\)00291-0](http://dx.doi.org/10.1016/S0017-9310(02)00291-0)

Creative Commons licensing terms

Author(s) will retain the copyright of their published articles agreeing that a Creative Commons Attribution 4.0 International License (CC BY 4.0) terms will be applied to their work. Under the terms of this license, no permission is required from the author(s) or publisher for members of the community to copy, distribute, transmit or adapt the article content, providing a proper, prominent and unambiguous attribution to the authors in a manner that makes clear that the materials are being reused under permission of a Creative Commons License. Views, opinions and conclusions expressed in this research article are views, opinions and conclusions of the author(s). Open Access Publishing Group and European Journal of Social Sciences Studies shall not be responsible or answerable for any loss, damage or liability caused in relation to/arising out of conflicts of interest, copyright violations and inappropriate or inaccurate use of any kind content related or integrated into the research work. All the published works are meeting the Open Access Publishing requirements and can be freely accessed, shared, modified, distributed and used in educational, commercial and non-commercial purposes under a [Creative Commons Attribution 4.0 International License \(CC BY 4.0\)](https://creativecommons.org/licenses/by/4.0/)